Brain Hemorrhages 1 (2020) 65–74

Contents lists available at ScienceDirect

Brain Hemorrhages

journal homepage: www.keaipublishing.com/en/journals/brain-hemorrhages/

Temporal evolution of heme oxygenase-1 expression in reactive astrocytes and microglia in response to traumatic brain injury

Alexander Morita [a], Amandine Jullienne [a], Arjang Salehi [a], Mary Hamer [a], Emon Javadi [a], Yasir Alsarraj [a], Jiping Tang [b], John H. Zhang [b,c,d], William J. Pearce [b,e], André Obenaus [a,f,*]

[a] Department of Basic Sciences, Loma Linda University, Loma Linda, CA 92350, USA
[b] Department of Physiology and Pharmacology, Loma Linda University, Loma Linda, CA 92350, USA
[c] Department of Anesthesiology, Loma Linda University, Loma Linda, CA 92350, USA
[d] Department of Neurosurgery, Loma Linda University, Loma Linda, CA 92350, USA
[e] Center for Perinatal Biology, Loma Linda University, Loma Linda, CA 92350, USA
[f] Department of Pediatrics, University of California Irvine, Irvine, CA 92697, USA

ARTICLE INFO

Article history:
Received 21 January 2020
Accepted 29 January 2020
Available online 15 February 2020

Keywords:
Astrocytes
Heme oxygenase-1
Microglia
Traumatic brain injury

ABSTRACT

Heme oxygenase-1 (HO-1) is an inducible enzyme that catabolizes heme into biliverdin (which is converted to bilirubin), carbon monoxide, and free iron. HO-1 and its downstream molecules have antioxidant and anti-inflammatory functions, making the effects of HO-1 difficult to predict. It is unknown if HO-1 expression has neuroprotective or neurodegenerative sequelae after traumatic brain injury (TBI). In adult male mice, we quantitatively investigated HO-1 expression in reactive astrocytes and microglia in a controlled cortical impact (CCI) model of TBI at 1, 7, 14, and 30 days post-injury (dpi). Immunoglobulin G (IgG) staining for blood-brain barrier (BBB) permeability was significantly increased at 1 and 7 dpi in TBI mice compared to controls. HO-1 expression in astrocytes was significantly increased acutely and sub-acutely (1, 7, 14 dpi) compared to controls. Significantly elevated expression of HO-1 in microglia was only observed at 14 and 30 dpi relative to controls. HO-1 expression remained elevated at 30 dpi following TBI relative to controls. This study for the first time demonstrates that HO-1 is highly expressed in perilesional tissues after TBI, but primarily in cells that contribute to the neuroinflammatory response. Modulating HO-1 expression may provide a path to therapeutic intervention by enhancing the neuroprotective aspects of HO-1.

Summary statement:: Heme oxygenase-1 expression after traumatic brain injury in adult male mice occurs first in reactive astrocytes followed by dramatic increases in microglia adjacent to the injury site.

1. Introduction

Millions of cases of traumatic brain injury (TBI) occur worldwide each year, many of which result in hospitalization or death.[30] In the U.S., 1.7 million individuals are diagnosed with TBI annually, and 80% of those are treated in the emergency department and released without being admitted.[23] Rates for emergency department visits and hospitalizations resulting from TBI have increased from 1995 to 2009.[15] Despite its prevalence and economic impact, at the present time there are no treatment regimens available for TBI. The cellular and molecular injury cascades evoked by TBI have been described as a two-stage process and has been described to include metabolic alterations.[25,57]

The initial primary injury is defined at the moment of impact and involves direct mechanical damage to brain tissues, including deposition of extravascular blood into the parenchyma. The early consequences of injury then lead to rapid and sustained elevation of neuroinflammatory events and activation of glial cells.[47] This initial injury cascade is then followed by a slower evolving secondary injury cascade that is composed of pathological processes and includes events such as ischemia, metabolic derangements, coagulopathies and intracranial hypertension.[23] In the secondary

Abbreviations: AP-1, Activator protein-1; BBB, blood-brain barrier; GFAP, glial fibrillary acidic protein; Bach1, BTB and CNC Homology 1; HO, heme oxygenase; HIF-1, hypoxia-inducible factor-1; IgG, immunoglobulin G; IBA1, ionized calcium-binding adapter molecule 1; Nrf2, nuclear factor E2-related factor 2; NFκB, nuclear factor kappa B; TBI, traumatic brain injury.

* Corresponding author at: Department of Pediatrics, University of California Irvine, Hewitt Hall, Room 2066, Irvine, CA 92697, USA.
E-mail address: obenausa@uci.edu (A. Obenaus).

https://doi.org/10.1016/j.hest.2020.01.002
2589-238X/

injury phase, there is increased release of excitatory neurotransmitters as well as an activation of voltage-dependent Ca^{2+} and Na^{+} channels. The Ca^{2+} influx activates enzymes such as lipid peroxidases and phospholipases which increase the intracellular concentration of free fatty acids and free radicals. Other enzymes such as caspases and endonucleases alter the structure of membranes and DNA. These events in multiple cell types (neurons, glia, vascular etc.) lead to membrane degradation of cellular and vascular structures, via necrotic or apoptotic pathways.[57]

Numerous molecular targets have been investigated in efforts to minimize the secondary injury to cells within the brain. One such target that is uniquely positioned to TBI-induced injury are heme oxygenases (HO).[1] HO are enzymes that are ubiquitously expressed in the brain and catalyze the conversion of heme into biliverdin, carbon monoxide (CO), and free ferrous iron. They are also known to have a range of ancillary functions including anti-inflammation, anti-oxidation and anti-proliferation.[44] In the brain there are three known HO isozymes: HO-1 is an inducible isozyme, HO-2 is constitutively expressed in the brain. HO-3 is a protein related to HO-2 but product of a different gene, is expressed in the brain but has poor heme catalyst activity.[39] HO is primarily an endoplasmic reticulum-resident protein but has also been located in the nucleus of cultured fibroblast cells exposed to heme or hypoxia,[35] in the nucleus of astroglial cells exposed to glutamate,[34] and in the nucleus of endothelial cells and smooth muscle cells.[33]

The products of HO activation are known to have diverse consequences: biliverdin is converted through biliverdin reductase to bilirubin,[54] which has antioxidant properties by scavenging peroxyl radicals formed from oxidation of lipids.[53] While high levels of CO result in CO poisoning and lead to free radical formation and neuronal death,[37] at low concentrations CO was shown to inhibit pro-inflammatory cytokines.[43] Iron accumulation in the brain has been associated with neurotoxicity primarily by reacting with reactive oxygen species.[22] However, free ferrous iron also induces the expression of ferritin, an iron transporting protein, which limits the effects of iron-catalyzed oxidant damage to cells.[6] Here, we chose to focus only on HO-1 because it is the inducible isozyme of heme oxygenases and is part of the neuroinflammatory response to TBI. Moreover, levels of HO-2 have been shown to be unchanged between injured and uninjured wild-type mice after a CCI.[12]

HO-1 is induced by a number of stimuli including heme,[3] kainic acid,[38] amyloid beta,[26] dopamine,[7] and heat.[19] Transcriptional activators of HO-1 include nuclear factor E2-related factor 2 (Nrf2),[4] hypoxia-inducible factor-1 (HIF-1),[32] activator protein-1 (AP-1),[2] and nuclear factor kappa B (NFκB).[40] One transcriptional repressor of HO-1 is BTB and CNC Homology 1 (Bach1),[28] which forms a heterodimer with a Maf protein. Thus, HO-1 is activated in response to a wide range of physiological and cellular stressors.

Few studies have assessed the temporal expression of HO-1 after TBI. Fluid percussion-induced brain injury in the rat induced HO-1 expression at one day after mild injury in macrophages in areas of hemorrhage including the subarachnoid space, and cortical glia.[20] With increasing TBI severity, HO-1 was detected in additional areas of hemorrhage such as the external capsule, hippocampus, and cerebellum.[20] In a cortical stab wound injury model, there were HO-1^{+} hypertrophic astrocytes as early as 12 h after injury and peaked at 3 dpi.[17] Park and colleagues found expression of HO-1 in astrocytes 4 days after cortical stab wound injury.[46] HO-1^{+} macrophages were reported between 1 and 3 dpi and persisted to at least 14 dpi.[17] In a rat weight-drop TBI model, increased numbers of HO-1^{+} microglia/macrophages were observed in the lesion and perilesional areas from 18 h post-injury to a maximum level at 96 h post-injury.[36] Thus, in TBI there is a robust expression of inducible HO-1 in response to injury but neither these responses nor the presence of HO-1 have been quantified temporally in glial cells.

HO-1 has also been observed in human tissues after TBI.[9] On autopsy, ramified and round cells at the lesion border were found as early as 24 h and up to 6 months post TBI. Most of the HO-1^{+} cells co-expressed CD68, a macrophage marker. Astrocytes weakly expressing HO-1 were observed up to 16 dpi while neurons appeared to express HO-1 at earlier time points (6 h to 7 dpi) adjacent to the lesion site.[42] HO-1 has also been detected in the cerebrospinal fluid from infants and children after severe TBI, where increased HO-1 concentrations were associated with increased injury severity and unfavorable neurological outcomes.[16]

Our study on HO-1 is the first report using controlled cortical impact (CCI) model of TBI. The advantage of the CCI model is that mechanical factors such as impact duration, velocity and depth can be controlled, as well as lack of risk of a rebound injury.[58] As described above, previous studies have noted increased HO-1 after TBI[9,18,20] in a range of cell types, but there is a lack of understanding of the temporal distribution of HO-1 in these cell types. Our hypothesis is that HO-1 is differentially expressed in reactive astrocytes and microglia after TBI. Given HO-1's anti-inflammatory and antioxidant properties, we sought to fill this knowledge gap by temporally quantifying HO-1 expression in astrocytes, microglia and neurons in mice at 1, 7, 14, and 30 days after a moderate CCI model of TBI. Our results can provide the basis for putative therapeutic intervention to mitigate the adverse outcomes observed in TBI.

2. Materials and methods

2.1. Animals

All animal experiments and care complied with federal regulations and were approved by the Institutional Animal Care and Use Committee. Adult male C57Bl/6J mice (N = 26, 8-week-old, 25 g, Jackson laboratory, Bar Harbor, ME) were group-housed in cages on a 12-hour light-dark cycle at constant temperature and humidity. All animals were randomly assigned to five experimental groups: controls (N = 4), TBI 1 dpi (N = 6), 7 dpi (N = 4), 14 dpi (N = 6), and 30 dpi (N = 6). A separate cohort was generated for tissue sections stained with IgG where male C57Bl/6J mice (N = 13, 6–7-month-old, 20–30 g, Jackson Laboratories) were randomly assigned to 2 groups: Sham or TBI. There were N = 4 sham males, euthanized 1-day post-surgery. The TBI groups were euthanized 1 dpi (N = 4) or 7 dpi (N = 5).

2.2. Controlled cortical impact TBI model

A CCI model of moderate brain injury was performed as previously described.[49] Briefly, mice were anesthetized (isoflurane 3% induction, 1.5% maintenance; Webster Veterinary Supply, Inc., Sterling, MA) and placed in a mouse stereotaxic frame (David Kopf Instruments, Tujunga, CA), with a heating pad that maintained body temperature at 37 °C. Lidocaine (lidocaine hydrochloride 2%) was injected subcutaneously at the scalp incision site. A midline incision was performed to expose the skull surface of anesthetized mice and a 5 mm craniotomy was performed, centered 2.5 mm posterior and 2.5 mm lateral from Bregma on the right side.

A moderate CCI (3 mm diameter tip, 1.5 mm depth, 2.0 m/s speed, 200 ms dwell) was delivered to the cortical surface using an electromagnetically driven piston (Leica Microsystems Company, Richmond, IL). The skin was sutured and buprenorphine (0.01 mg/kg, intramuscular) was administered after surgery to minimize pain. Control animals were anesthetized for the identical

period of time as injury animals and administered buprenorphine. Injured animals were randomly selected and euthanized at the selected time points (1, 7, 14, 30 days). Control animals (only administered isoflurane and buprenorphine) were euthanized at 3 days after exposure. Sham animals went under the same procedure as injured animals but without cortical impact and were euthanized 1 day post-surgery.

2.3. Immunohistochemistry

Animals were sacrificed by transcardial perfusion with phosphate buffered saline (PBS) and 4% paraformaldehyde (PFA). Prior to cryosectioning brains were placed in 30% sucrose and embedded in optimal cutting temperature compound (O.C.T. Compound, #4583, Tissue Tek; Sakura Fine Tek, Torrance, CA). 25 μm-thick coronal sections were cut using a Leica CM1850 cryostat (Leica Microsystems GmbH, Wetzlar, Germany), mounted directly on microscope slides (Fisherbrand™ Superfrost Plus Microscope Slides, #12-550-15, Fisher Scientific, Pittsburgh, PA) and kept at -20 °C.

Mounted sections were labeled with anti-rabbit HO-1 (1:200, Enzo Life Sciences Cat# ADI-SPA-895, Farmingdale, NY, RRID: AB_10618757), incubated in PBS + 0.5% bovine serum albumin (BSA) at room temperature overnight.

Sections were simultaneously labeled with either anti-mouse glial fibrillary acidic protein (GFAP; 1:500, EMD Millipore Cat#-MAB3402, Burlington, MA, RRID: AB_94844), anti-goat allograft inflammatory factor 1 (AIF-1)/ionized calcium-binding adapter molecule 1 (Iba1; 1:200, Novus Biologicals Cat#NB100-1028, Littleton, CO, RRID: AB_521594), or anti-mouse neuronal-specific nuclear protein (NeuN; 1:800, EMD Millipore Cat#MAB377, Burlington, MA, RRID: AB_2298772) at room temperature overnight. Sections were then incubated with the right combination of secondary antibodies: goat anti-rabbit Alexa Fluor® 594 (1:1000, Thermo Fisher Cat #A-11012, Waltham, MA, RRID: AB_2534079) or donkey anti-rabbit Alexa Fluor® 594 (1:1000, Thermofisher Cat#A-21207, RRID: AB_141637), and goat anti-mouse Alexa Fluor® 488 (1:1000, Thermo Fisher Cat#A-11029, RRID: AB_2534088) or donkey anti-goat Alexa Fluor® 488 (1:1000, Thermo Fisher Cat#A-11055, RRID: AB_2534102) for 1.5 hours. For IgG staining, sections were incubated with anti-mouse IgG-fluorescein isothiocyanate (FITC) antibody (1:200, Sigma-Aldrich #F0257, Burlington, MA, RRID: AB_259378) at room temperature overnight. Sections were coverslipped by using Vectashield HardSet Antifade Mounting Medium with DAPI (Vector Laboratories #H-1500, Burlingame, CA, RRID: AB_2336788).

2.4. Microscopy

A BZ-X700 Keyence microscope (Keyence Corp, Elmwood Park, NJ) was used to acquire the images using Z-stacks of the coronal sections using 1 μm steps encompassing 25 slices and resulting in a 25 μm slab. Following acquisition, BZ-II Analyzer software (Keyence Corp, Elmwood Park, NJ, RRID: SCR_016348) was used to merge Z-stacks into full focus images.

Image processing included adjustment of brightness and contrast for each of the acquired images. 2× images of the whole brain slice were obtained by using the XY-stitching function. Image correction using black balance was performed only for tissue stained with the anti-IgG antibody.

2.5. Histological measurements

In order to determine tissue loss as a result of TBI, 2× images of the entire brain slice were acquired to measure the brain area on both right and left hemispheres. Using ImageJ software (National Institutes of Health, Rockville, MD, RRID: SCR_003070), regions of interest (ROI) for both right and left hemispheres were drawn by a blinded experimenter (Fig. 1A). Areas were measured to compare the difference between the ipsilateral and contralateral hemispheres to obtain a ratio (ipsilateral area: contralateral area) where a decreased ratio would denote TBI severity.

To evaluate BBB disruption, IgG images (2×) were analyzed by a blinded experimenter using ImageJ software, where integrated density measurements were performed on the top right quarter of the brain that contained the lesion site (Fig. 3A).

2.6. Quantification of cell counts

Two 20× images of the cortex (Fig. 1B) adjacent to the lesion (−1.70 to −1.90 mm relative to Bregma) were analyzed independently by 2 blinded experimenters using Image-Pro Premier software (v9.1, Media Cybernetics, Rockville, MD, RRID: SCR_016497). The brightness of the color channels (red for HO-1, green for GFAP or Iba-1) were minimized to remove background and values of the brightness were recorded.

A colocalization mask of the red and green colocalized pixels was used to create a composite image with the blue channel for DAPI staining. Thresholds for the red and green color channels were normalized to the recorded brightness measurements. To determine the number of astrocytes ($GFAP^+$) or microglial cells ($Iba1^+$) stained with HO-1, $DAPI^+$ cells containing colocalized pixels were counted by manual tagging. $DAPI^+$ cells with less than 75% overlap with the colocalized pixels were not counted. Cell counts from the two images were then averaged to a single value. The personnel conducting the cell counts were blinded to the treatment conditions.

2.7. Statistics

One-way analysis of variance (ANOVA), Tukey's multiple comparisons tests were performed using GraphPad (GraphPad Prism 7.0, San Diego, CA, RRID: SCR_002798). The data for the parametric tests exhibited a normal distribution and passed the Shapiro-Wilk normality tests. Values are presented as mean ± SEM with statistical significance reported at $^*p < 0.05$, $^{**}p < 0.01$, $^{***}p < 0.001$ and $^{****}p < 0.0001$. Outliers were removed if they were above or below 1.5 times the interquartile range (IQR).

3. Results

Although all animals survived the TBI procedure, there were significant differences in body weight in animals over the 30d time course between TBI and control mice. There was no significant difference between pre-surgery and post-surgery weights for 1 dpi (Paired t-test, p = 0.46) and 7 dpi (Paired t-test, p = 0.20) mice. There was a significant increase in weights between pre-surgery and post-surgery for 14 dpi (Paired t-test, p = 0.05) and 30 dpi (Paired t-test, p < 0.01) mice. There was no significant difference in control animals that were only administered with isoflurane and sacrificed (Paired t-test, p = 0.34).

3.1. Tissue loss and BBB disruption and total HO-1^+ cell counts

To characterize the relationship between TBI and HO-1, we assessed tissue loss and BBB disruption as well as the total numbers of HO-1^+ cells after TBI. We measured ipsilateral and contralateral tissue area and IgG staining of brain tissue. In the ipsilateral hemisphere, there was progressive tissue loss that became significant 30 dpi (87.24 ± 0.02% remaining) compared to control mice (97.94 ± 0.01% remaining; $^*p = 0.013$; Fig. 1C). At 1 dpi, cells expressing HO-1 appeared to be primarily astrocytes

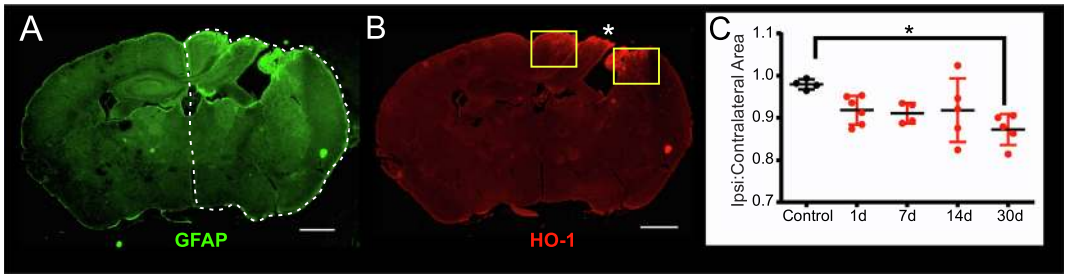

Fig. 1. Tissue loss after TBI. (A) Lesion area following moderate TBI was derived from GFAP stained tissue sections comparing ipsilateral (dotted white line) and contralateral hemispheres as a ratio for injured tissue (see C). (B) Two perilesional cortical regions (yellow boxes) adjacent to the lesion but excluding regions of frank tissue loss were analyzed for quantification of HO-1$^+$ microglia and astrocytes. Asterisk indicates site of injury. (C) Lesion area was quantified at each time point after injury. Despite tissue heterogeneity there was a sustained loss of tissue on the ipsilateral brain at 30 dpi. (*p < 0.01, Scale bars = 1 mm for A, B.

and microglia, but no overt colocalization in neurons was observed in the perilesional cortex (Fig. 2A–C). The number of HO-1$^+$ cells (colocalized with DAPI) was significantly increased between 7 dpi (311.60 ± 51.02 cells; *p = 0.03) and 14 dpi (298.20 ± 30.63 cells; *p = 0.03) vs controls (91.50 ± 41.04 cells). There was no significant difference between 1 dpi (275.00 ± 45.54 cells; p = 0.06), 30 dpi (239.20 ± 43.93 cells; p = 0.21) and control (91.50 ± 41.04 cells; Fig. 2D).

Evaluation of BBB integrity using IgG staining showed an increased permeability at 1 dpi that was resolved by 7 dpi (Fig. 3B–E). BBB quantification in the injured hemisphere revealed significantly increased staining density in 1 dpi (803.83 ± 147.47; ***p = 0.001) and 7 dpi mice (679.60 ± 337.27; ***p = 0.0043) compared to sham controls (136.49 ± 55.38; Fig. 3F). BBB disruption was significantly reduced at 14 dpi (211.87 ± 82.23; **p = 0.004), and 30 dpi (49.84 ± 9.45; ****p = 0.0004) compared to 1 dpi. There was also a significant decrease between 7 and 30 dpi (**p = 0.002; Fig. 3F). The BBB in our model of TBI is disrupted at 1 and 7 dpi but this perturbation recovers to control levels by 14 and 30 dpi.

3.2. HO-1 colocalization in astrocytes

Immunostaining for HO-1 and GFAP at 1–30 dpi revealed significant increases in HO-1 and GFAP colocalization (Fig. 4A–E). The expression of HO-1$^+$ astrocytes appeared in a sub-population of astrocytes as not all GFAP$^+$ cells expressed HO-1. Compared to control mice (1.75 ± 0.47 cells), significant increases in the number of perilesional astrocytes co-localizing HO-1 at 1 dpi (35.33 ± 6.25 cells; **p = 0.006), 7 dpi (47.50 ± 3.52 cells; ****p < 0.0001), and 14 dpi (33.60 ± 4.88 cells; **p = 0.002) were observed. The number of HO-1/GFAP colocalized cells significantly decreased from 7 dpi (47.50 ± 3.52 cells) to 30 dpi (22.50 ± 2.53 cells; *p = 0.02; Fig. 4F). It is apparent that not all astrocytes express HO-1, as evidenced by the lack of HO-1 staining in some GFAP$^+$ cells (Fig. 4C-D).

3.3. HO-1 colocalization in microglia

Immunostaining for HO-1 and Iba1 over the same time course also displayed a robust increase in HO-1 and Iba1 colocalization

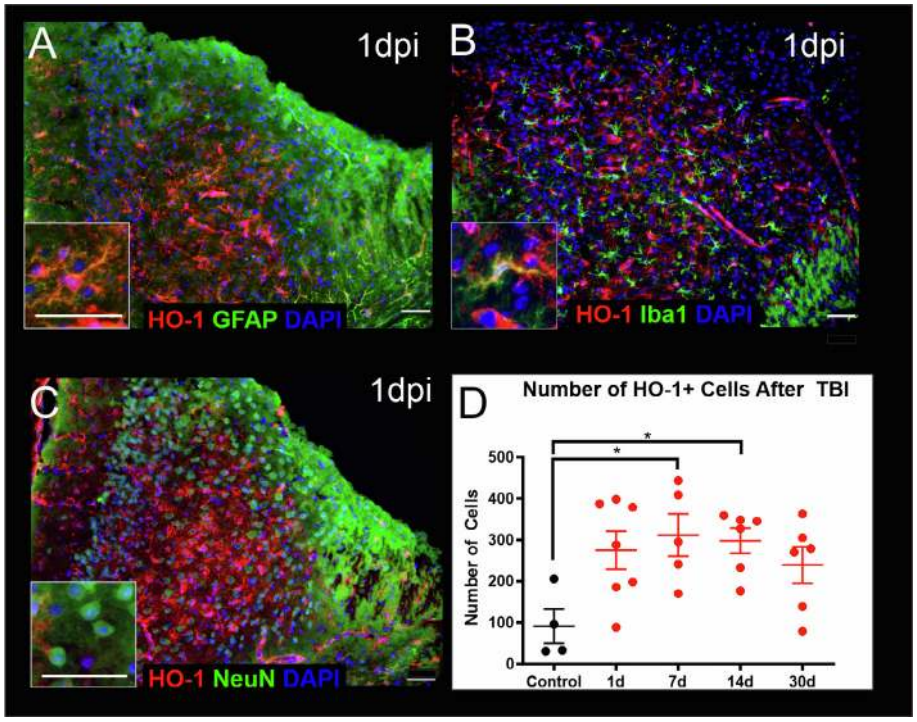

Fig. 2. Cell types expressing HO-1 and the temporal evolution of total HO-1$^+$ cells after TBI. (A) Perilesional cortex at 1 dpi illustrating HO-1 and GFAP immunostaining where a subset of GFAP$^+$ cells express HO-1. (B) Iba1$^+$ microglia and HO-1 in the perilesional cortex at 1 dpi were also colocalized. (C) In contrast, there was a lack of neuronal (NeuN) and HO-1 colocalization in the perilesional cortex. (D) The number of HO-1$^+$ cells increased over 7 dpi but remained elevated relative to controls at 30 dpi (Control vs 7 dpi *p < 0.03, control vs 14 dpi *p < 0.03). Scale bars = 50 μm for A–C.

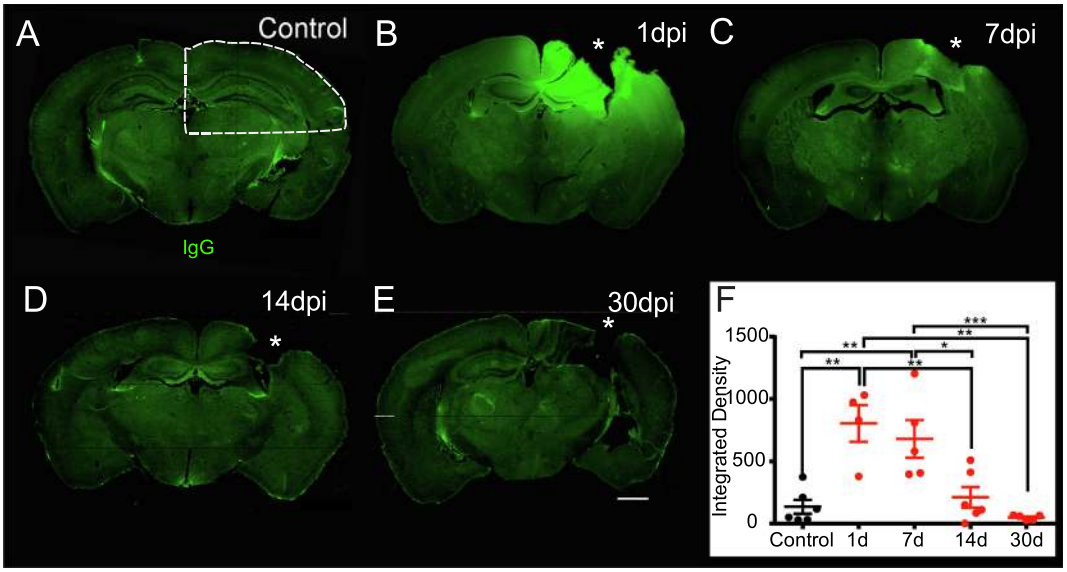

Fig. 3. Temporal evolution of blood-brain barrier integrity (BBB) after TBI. (A) Blood-brain barrier (BBB) integrity after TBI was assessed using IgG staining. Staining in controls (shams) did not exhibit any IgG leakage. Dotted line illustrates the region used for quantification of BBB leakage following TBI. (B) IgG staining was dramatically increased in the ipsilateral cortex and hippocampus of mice at 1 dpi (* = site of TBI). (C) Moderate, but reduced IgG was still visible at 7 dpi. (D) At 14 dpi there was minimal IgG leakage evident in the majority of TBI mice. (E) BBB leakage at 30 dpi was not found in the cortex of the ipsilateral hemisphere. (F) Quantification (integrated densities, a.u.) of IgG staining at the injury site revealed significantly increased BBB disruption at 1–7 dpi with a return to control levels by 30 dpi (control vs. 1 dpi $^{**}p < 0.001$, control vs. 7 dpi $^{**}p < 0.004$, 1 dpi vs. 14 dpi $^{**}p < 0.003$, 1 dpi vs. 30 dpi $^{***}p < 0.004$, 7 dpi vs. 14 dpi $^{*}p < 0.02$, 7 dpi vs. 30 dpi $^{**}p < 0.001$). Scale bar for all images = 1 mm.

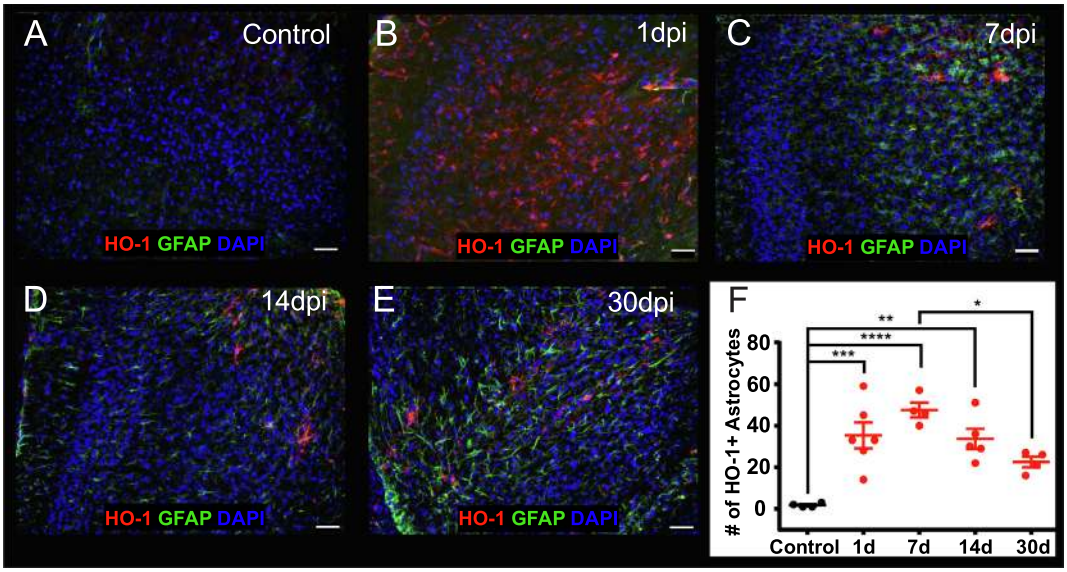

Fig. 4. HO-1 expression in astrocytes following TBI. HO-1 and GFAP colocalization in the ipsilateral perilesional cortex of control and injured mice (20× magnification) from control (A) and TBI mice at 1 dpi (B), 7 dpi, (C) 14 dpi, (D) and (E) 30 dpi. (F) Quantification of HO-1$^+$ GFAP astrocytes demonstrated increased colocalization that peaks at 7 dpi but remains elevated at 30 dpi relative to uninjured controls. Each data point represents the total number of colocalized cells for one animal. ($^{*}p < 0.004$, $^{**}p < 0.001$, $^{***}p < 0.0002$). Scale bars = 50 μm.

(Fig. 5A–E). There was a significant increase in HO-1$^+$ and Iba1 cells between controls (25.5 ± 9.53 cells) and 14 dpi (228.33 ± 29.55 cells; $^{***}p = 0.001$) and 30 dpi (147.33 ± 36.25 cells; $^{*}p = 0.0245$). There was also a significant increase in HO-1$^+$ microglial cells between 1 dpi (57.14 ± 5.78 cells) and 14 dpi (228.33 ± 29.55 cells; $^{***}p = 0.0002$), and between 7 dpi (103.6 ± 19.93 cells) and 14 dpi (228.33 ± 29.55 cells; $^{*}p = 0.0124$; Fig. 5F). Similar to astrocytes, there was a sustained elevation of HO-1$^+$ microglia even at 30 dpi.

3.4. Comparisons of HO-1 colocalization in astrocytes and microglia

In examining the temporal evolution of HO-1$^+$ cells between astrocytes and microglia it was clear that there were a higher number of microglial cells expressing HO-1, particularly at the later time points. In comparisons across all time points, we found significantly increased numbers of HO-1$^+$ microglia (228.33 ± 29.55) at 14 dpi compared to HO-1$^+$ astrocytes at the same time point (33.60 ± 4.88 cells; $^{****}p < 0.0001$) (see Figs. 4 and 5). Similarly, at

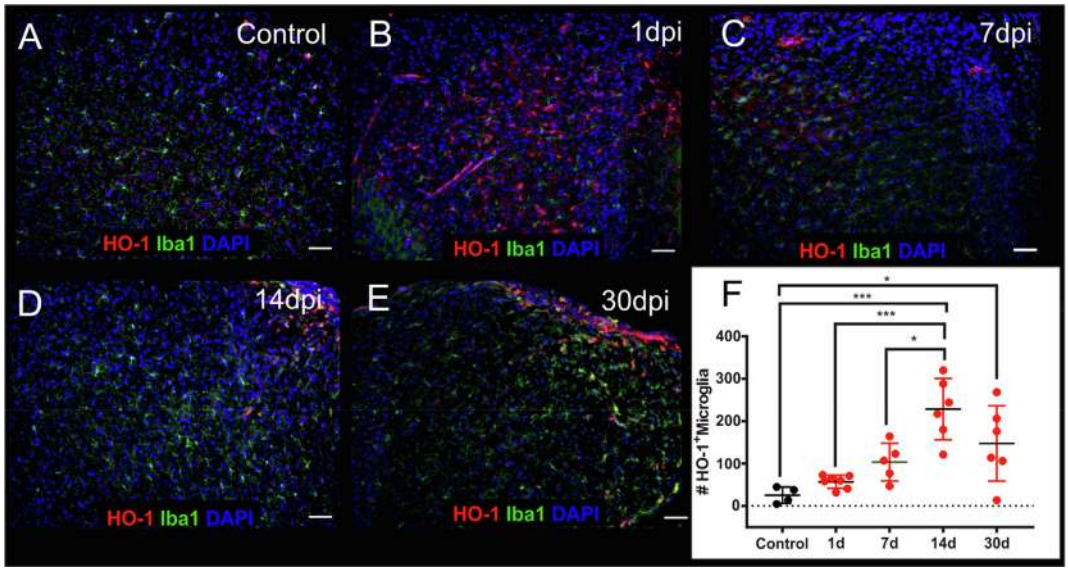

Fig. 5. HO-1 expression in microglia following TBI. Co-immunostaining for HO-1 and Iba1 in the ipsilateral perilesional cortex of control and injured mice. Photomicrographs of perilesional cortex adjacent to the lesion in control (A), 1 dpi (B), 7 dpi (C), 14 dpi (D), 30 dpi (E) mice following a moderate TBI. (F) Quantification of HO-1$^+$ and Iba1 colocalization identified that HO-1$^+$ microglia peak at 14 dpi and remain elevated at 30 dpi. Note that the number of HO-1$^+$ microglia never return to control levels. Each data point represents the total number of colocalized cells for one animal. (**p < 0.01, ***p < 0.001, ****p < 0.0001). Scale bars = 50 μm.

30 dpi there were significantly increased numbers of HO-1$^+$ microglia (147.33 ± 36.25 cells) relative to HO-1$^+$ astrocytes (22.50 ± 2.53 cells; ****p < 0.0001).

3.5. Morphological comparisons of HO-1 colocalization in astrocytes and microglia

Astrocyte morphology is altered in mild to severe reactive astrogliosis.[51] In severe injury, diffuse reactive astrogliosis results in pronounced hypertrophy of cell body and processes with crossing of neighboring astrocyte processes resulting in blurring and disruption of individual astrocyte domains.[51] Some astrocytes expressing HO-1 at 1 dpi appeared to be of the reactive subtype (Fig. 6A). At 7 dpi the astrocytes that colocalized HO-1 possessed thicker processes extending from more pronounced hypertrophic cell bodies which were still observed at 14 dpi (Fig. 6A). In microglia, HO-1 expression was found in round-shaped microglia with long processes at 1 dpi (Fig. 6B) but by 7 dpi HO-1$^+$ microglia appeared to be swollen with contracted processes, indicative of an ameboid morphology (Fig. 6B).

3.6. Temporal aspects of HO-1 expression

Comparison of the temporal evolution of HO-1$^+$ astrocytes and microglia demonstrated that HO-1$^+$ microglia peaked at 14 dpi while astrocytic numbers were maximal at 7 dpi, with 27-fold increase above controls (Fig. 7A). The number of HO-1$^+$ astrocytes was reduced by 14 dpi but did not return to control levels by 30 dpi, where it remained elevated 13-fold more than controls. The number of microglia expressing HO-1 reached a 9-fold peak over controls at 14 dpi was still elevated and remained 6-fold over controls. This novel finding would suggest a sustained level of HO-1 expression in inflammatory microglial cells in perilesional tissues even at chronic periods after TBI.

The estimated percentage of HO-1$^+$ GFAP$^+$ cells out of the total number of HO-1$^+$ cells in the experimental groups ranges from 7.65 ± 4.82 % (controls) to a maximum of 25.08 ± 11.89% at 14 dpi (Fig. 7B). The estimated percentage of HO-1$^+$ Iba1$^+$ cells out of the total number of HO-1$^+$ cells in the experimental groups ranged from 23.35 ± 2.90 % (1 dpi) to a maximum of 76.57 ± 6.03 % at 14 dpi (Fig. 7B). Both the actual number of and the relative percentage HO-1$^+$ cells followed a virtually identical temporal pattern of expression after TBI within the perilesional cortex.

4. Discussion

HO-1 expression is increased in various types of acquired neurological injuries. In TBI there have been no reports of the quantitative distribution of HO-1$^+$ glial cells. While astrocytes and microglia are glial cells, they are distinct cells and express different levels of HO-1 over time. Astrocytes are derived from neural stem cells, which also give rise to neurons.[5] Microglia are derived from yolk sac macrophages that seed the brain during early development, and embryonic microglia grow and span the entire CNS until adulthood.[24] We describe for the first time the temporal evolution of perilesional HO-1 expression in reactive astrocytes and microglia following a moderate TBI injury in adult male mice. We did not observe HO-1 in neurons, suggesting that it is not induced in this cellular population in response to TBI. However, we observed a high level of HO-1 expression in microglia that peaked at 14 dpi, but which remained elevated at 30 dpi compared to control levels. Astrocytic HO-1 expression was significantly lower than that of microglia, following a more gradual pattern of increases, peaking at 7 dpi and decreasing by 30 dpi. Notably, the HO-1 response in both astrocytes and microglia was still elevated (relative to controls) at 30 dpi consistent with the hypothesis of ongoing chronic inflammation after TBI. Our novel study is the first to quantitatively and temporally examine HO-1 in glial cells over the course of 30 days following TBI.

Our observation of virtually no HO-1 expression in neurons in our study and predominately in astrocytes and microglia is consistent with a previous study where Chang and colleagues performed CCI in HO-2 knockout mice.[12] They found that HO-2 was detected in neurons throughout the brain but HO-1 was detected only in glial cells. Other studies have on occasion described minimal HO-1 expression in neurons but not contributing greatly to overall HO activity. Liu and colleagues found HO-1 expression in neurons in the ipsilateral cortex after weight-drop induced-TBI in rats, but

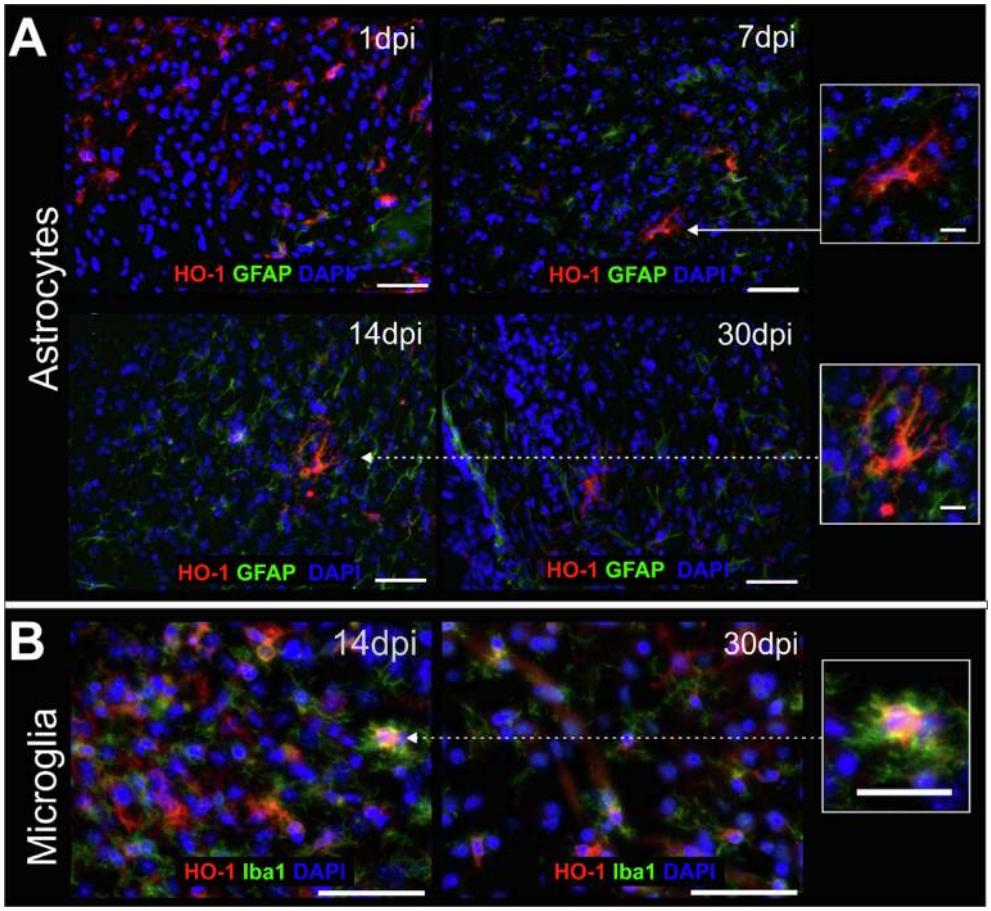

Fig. 6. Morphologic comparisons of HO-1$^+$ expressing cells. (A) Astrocytes expressing HO-1 appeared stellate in shape at 1 dpi which by 7 dpi expressed a hypertrophied morphology with thickened processes (see inset to right). The astrocytic hypertrophic appearance was still present at 14 dpi (see inset to right) but by 30 dpi astrocyte numbers were reduced and were more amoeboid in morphology. (B) Microglia expressing HO-1 at 14 dpi expressed an amoeboid morphology that were not observed at 30 dpi. Scale bar = 50 μm; inset scale bar = 25 μm.

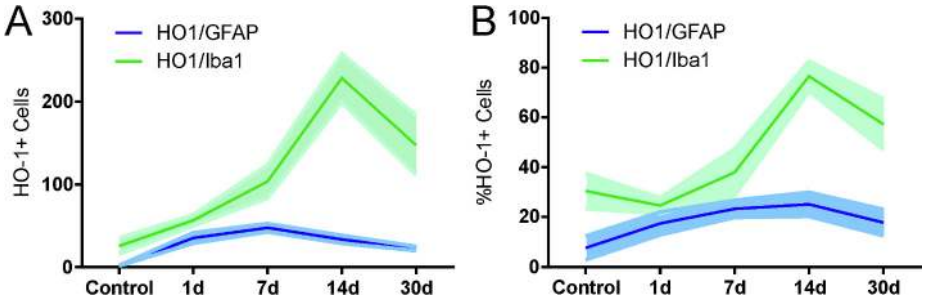

Fig. 7. Temporal evolution of colocalization of HO-1 with glial cells. (A) Number of HO-1$^+$ astrocytes (solid blue line) and microglia (solid green line) in the perilesional cortex over time after moderate TBI, illustrating that HO-1$^+$ microglia peak at 14 dpi. However, both astrocytes and microglia have a sustained level of co-expression within the perilesional cortex. Lighter shaded lines indicate S.E.M. (B) The percentage of GFAP$^+$ (solid blue line) and Iba1$^+$ cells (solid green line) expressing HO-1 over the total number of HO-1$^+$ cells over time after TBI confirm a similar pattern of expression. Lighter shaded lines indicate S.E.M.

this level of expression was not significantly different compared to the contralateral cortex.[36] These findings, including our own, would suggest that HO-1 expression is predominantly restricted to glial cells after TBI. However, neuronal expression of HO-1 has been reported in primary cultures of ventral mesencephalon neurons after treatment with oxidative stress inducer mitochondria complex 1-methyl-4-phenylpyridinium where the authors noted that HO-1 expression was induced earlier in cultured astrocytes, hinting that it might be more efficiently expressed in glial cells than in neurons.[60]

HO-1 expression in the developing rat brain has been shown to change over time with widespread expression in multiple regions of the brain in P7 rats and intense in regions of myelinogenesis of white matter.[8] In adult rats, the expression profile was increased in areas such as hypothalamus and the dentate gyrus. HO-1 was detected in microglia-like cells and neurons in the cortex which decreased with age.[8] In our study we did not detect overt HO-1 staining in the cortex of adult uninjured animals (Figs. 4A and 5A). The expression of HO-1 in its role in neonatal or juvenile TBI has not been studied. Future work should investigate if there is a

difference in HO-1 expression in younger animals after TBI, and a potential area of interest could be myelin, which has been shown to be modified after juvenile TBI.[31] Myelin basic protein has been reported to induce expression of HO-1 in human astroglial cells.[10]

The predominant expression of HO-1 in microglia is similar to those observed by Liu and colleagues[36] in a rat open-skull weight-drop induced-TBI model. They detected significantly increased HO-1$^+$ microglia in the cortex as early as 18 h post-injury and up through 96 h post-injury compared to controls. While we observed HO-1$^+$ microglia at 1 dpi the numbers of microglia expressing HO-1 only became significant at 14 dpi. However, surprisingly in contrast to our findings, Liu and colleagues did not detect GFAP$^+$ HO-1$^+$ cells in their study. We found that HO-1$^+$ astrocytes were observed early, but in general, HO-1 was expressed primarily in microglia following moderate TBI. HO-1 expression in microglia at 3 days after a fluid percussion injury in rats found that HO-1 is mainly expressed in astrocytes,[21] which was confirmed in a lateral fluid percussion injury.[59] Differences between TBI models may highlight contrasting mechanisms of HO-1 expression and the level of subsequent inflammation. As, such, the model of injury should be taken into consideration when interpreting outcomes.

HO-1 expression in microglia has also been reported in other types of brain injury. Hyperosmotic opening of the BBB induced expression of HO-1 in astrocytes and microglia.[48] HO-1 expression in microglia/macrophages was detected 24 h after collagenase-induced intracerebral hemorrhage in mice.[56] These studies combined with our own, clearly demonstrate that the function of microglial HO-1 after brain hemorrhage may act to prevent or limit neuronal death.

Schallner and colleagues demonstrated that deletion of HO-1 in microglia reduced erythrophagocytosis but increased neuronal apoptosis after subarachnoid hemorrhage.[50] Thus, hemorrhagic events as in TBI would advocate that HO-1 may have a similar function as that reported in intracerebral/subarachnoid hemorrhage, but additional studies need to be undertaken to definitively evaluate the role of HO-1$^+$ microglia after TBI.

In contrast to the late expression of microglia, we found that astrocytes expressed HO-1 as early as 1 dpi and continued through 30 dpi. In a cortical stab wound model, HO-1$^+$ astrocytes were observed as early as 12 h post-injury that declined by 3 dpi near the wound area in rats.[18] HO-1$^+$ astrocytes have also been observed after fluid percussion TBI.[21] Recently, we reported sex differences in HO-1 expression in TBI where increased HO-1 expression was observed in the injured cortex in female mice at 1 dpi but not males.[27] Curiously, HO-1$^+$ astrocytes were not observed after weight drop injury in rats but this may reflect the relative severity of the injury.[36] It is clear that the role of increased HO-1 expression in astrocytes remains to be clarified in TBI.

An interesting observation of our study was the time at which HO-1$^+$ expression in astrocytes (7 dpi) and in microglia (14 dpi) peaked. Previous CCI TBI studies have reported peak expression of GFAP and OX-42 (a microglia/macrophage marker) at 4 dpi[14] and in C57BL/6 mice astrogliosis peaked at 3 dpi.[55] These findings, in combination with our results, would suggest that the level of HO-1 expression does not necessarily coincide with peak astrocyte or microglia activation in the injured cortex. Villapol and colleagues noted that the peak level of apoptosis in the perilesional cortex was 5 hours post-injury and this high level persisted through 3 dpi.[55] A cell culture study on mouse neurons overexpressing HO-1 found that increased levels of HO-1 resulted in decreased cell death when exposed to glutamate.[13] The physiological significance of temporal HO-1 expression patterns in astrocytes and microglia requires future study, particularly as it relates to the known inflammatory responses of these cells in TBI.

It is important to note that not all the HO-1$^+$ cells expressed either GFAP or Iba1. The total number of colocalized cells (HO-1/GFAP, HO-1/Iba1) only contributed to about 30% of the cells for the control animals, 33% of the total HO-1$^+$ cells at 1 dpi and 49% at the 7 dpi within the perilesional cortex (Fig. 7B). The percentage of HO-1$^+$ glial cells increased to 87% at 14 dpi and slowly subsided to 70% at 30 dpi. GFAP is a marker for reactive astrocytes, but it has been shown that many mature astrocytes in healthy CNS tissue do not express detectable levels of GFAP.[51] Other potential astrocyte markers include S100β or ALDHL1 (Aldehyde dehydrogenase 1 family, member L1). S100β has been described to be expressed in astrocytes, but has been shown in studies not to be astrocyte-specific, staining oligodendrocytes and lymphocytes.[52] ALDHL1, has been described as an astrocyte specific marker, and has been shown to label more astrocytes than GFAP staining.[11] Future studies utilizing these additional astrocytic markers could enhance our understanding of whether non-reactive glial cells also express HO-1 in response to TBI. Endothelial cells are another cell type that may express HO-1 after TBI, as reported in cultured cerebral microvascular endothelial cells[45] and in endothelial cells after middle cerebral artery occlusion.[41]

Differences in TBI models and injury severity may underlie some of the reported differences between studies. In contrast to our own findings wherein we observed increased GFAP staining as early as 1 dpi (Fig. 2B), Villapol and colleagues did not observe any signs of astrogliosis at early time points following a milder form of TBI.[55] Chen and colleagues were able to detect expression of GFAP as early as 1 dpi using severe CCI model in rats.[14] In our model of moderate TBI, at 7 dpi we observed robust HO-1 expression in a subset of astrocytes (Fig. 4) with diminution over 30 dpi, but with HO-1$^+$ astrocytes present at later time points (Figs. 4 and 7). In our study, the elevation in HO-1$^+$ astrocytes and microglia appeared to be limited to the region around the necrotic lesion, similar to that of fluid percussion injury.[21]

There have been few studies examining molecular regulators of HO-1 expression after TBI. Park and colleagues found that Toll-like receptor 2 (TLR2) was necessary for glial cell activation and HO-1 expression in the stab wound injured mouse brain.[46] TLR2 knock-out mice exhibited reduced HO-1 expression after injury as well as decreased astrocyte and microglial activation, suggesting TLR2 may be a mediator of glial activation and HO-1 expression after TBI. Expression of TLR2, TLR4, MyD88 and HSP70 were detected after an open-skull weight drop injury.[61] Toll-like receptor signaling was also investigated after CCI by Krieg and colleagues where knock-out of TLR2 and TLR4 resulted in decreased contusion volume, increased interleukin (IL)-1β, and decreased IL-6 and HMGB1 (high mobility group box 1) compared to WT controls at early time points.[29] It would appear modulation of TLR signaling may be important in controlling HO-1 expression and possibly inflammation, but more long-term studies need to be done to establish a clear role in this signaling pathway after TBI.

There have been few studies investigating long-term expression of HO-1 after TBI. The first long-term study was done with human tissue, where HO-1 expression was prevalent as late as 6 months post injury.[9] Our results show that HO-1 is still expressed in astrocytes and microglia up to 30 days after CCI, which is in agreement with Chang and colleagues, where they detected HO-1 in microglia and astrocytes in areas next to the area of impact after using CCI in mice by 14 dpi.[12] The long-term presence of HO-1 in the brain after TBI play a significant role in TBI outcomes, possibly by modulating inflammation.

In conclusion, temporal HO-1 expression differs dramatically between astrocytes and microglia after TBI, highlighting the need to carefully assess these primary inflammatory cells in neurological injuries. Both HO-1$^+$ microglia and HO-1$^+$ astrocytes were

observed early after TBI but as the injury matured there were significantly higher levels of HO-1^{+} microglia. The maintained HO-1 expression in inflammatory cells may contribute to minimizing known microglial oxidative stress, as well as potentially limiting lesion expansion in response to cortical tissue injury in TBI. It remains to be determined if enhancing HO-1 expression in reactive astrocytes and microglia could promote an earlier and sustained morphological and functional recovery after TBI.

Author contributions

AM, AJ, AO Designed research; AM, AJ, AS, EJ, MH Performed research; AM, AJ, AS, MH, EJ, YA, AO Analyzed data; AM, AJ, JT, JHZ, WJP, AO Contributed to and reviewed the manuscript.

6. Declarations of interest

None.

Funding

This research project was supported by the National Institute of Neurological Disorders and Stroke grant P01NS082184.

References

1. Abraham NG, Junge JM, Drummond GS. Translational significance of heme oxygenase in obesity and metabolic syndrome. *Trends Pharmacol Sci*. 2016;37:17–36.
2. Alam J, Den Z. Distal AP-1 binding sites mediate basal level enhancement and TPA induction of the mouse heme oxygenase-1 gene. *J Biol Chem*. 1992;267:21894–21900.
3. Alam J, Shibahara S, Smith A. Transcriptional activation of the heme oxygenase gene by heme and cadmium in mouse hepatoma cells. *J Biol Chem*. 1989;264:6371–6375.
4. Alam J, Stewart D, Touchard C, Boinapally S, Choi AM, Cook JL. Nrf2, a Cap'n'Collar transcription factor, regulates induction of the heme oxygenase-1 gene. *J Biol Chem*. 1999;274:26071–26078.
5. Alvarez-Buylla A, Garcia-Verdugo JM, Tramontin AD. A unified hypothesis on the lineage of neural stem cells. *Nat Rev Neurosci*. 2001;2:287–293.
6. Balla J, Jacob HS, Balla G, Nath K, Eaton JW, Vercellotti GM. Endothelial-cell heme uptake from heme proteins: induction of sensitization and desensitization to oxidant damage. *PNAS*. 1993;90:9285–9289.
7. Berger SP, Hunger M, Yard BA, Schnuelle P, Van Der Woude FJ. Dopamine induces the expression of heme oxygenase-1 by human endothelial cells in vitro. *Kidney Int*. 2000;58:2314–2319.
8. Bergeron M, Ferriero DM, Sharp FR. Developmental expression of heme oxygenase-1 (HSP32) in rat brain: an immunocytochemical study. *Brain Res Dev Brain Res*. 1998;105:181–194.
9. Beschorner R, Adjodah D, Schwab JM, et al. Long-term expression of heme oxygenase-1 (HO-1, HSP-32) following focal cerebral infarctions and traumatic brain injury in humans. *Acta Neuropathol*. 2000;100:377–384.
10. Businaro R, Fabrizi C, Caronti B, Calderaro C, Fumagalli L, Lauro GM. Myelin basic protein induces heme oxygenase-1 in human astroglial cells. *Glia*. 2002;37:83–88.
11. Cahoy JD, Emery B, Kaushal A, et al. A transcriptome database for astrocytes, neurons, and oligodendrocytes: a new resource for understanding brain development and function. *J Neurosci*. 2008;28:264–278.
12. Chang EF, Wong RJ, Vreman HJ, et al. Heme oxygenase-2 protects against lipid peroxidation-mediated cell loss and impaired motor recovery after traumatic brain injury. *J Neurosci*. 2003;23:3689–3696.
13. Chen K, Gunter K, Maines MD. Neurons overexpressing heme oxygenase-1 resist oxidative stress-mediated cell death. *J Neurochem*. 2000;75:304–313.
14. Chen S, Pickard JD, Harris NG. Time course of cellular pathology after controlled cortical impact injury. *Exp Neurol*. 2003;182:87–102.
15. Coronado VG, McGuire LC, Sarmiento K, et al. Trends in Traumatic Brain Injury in the U.S. and the public health response: 1995–2009. *J Saf Res*. 2012;43:299–307.
16. Cousar JL, Lai Y, Marco CD, et al. Heme oxygenase 1 in cerebrospinal fluid from infants and children after severe traumatic brain injury. *Dev Neurosci*. 2006;28:342–347.
17. Dwyer BE, Nishimura RN, Lu SY. Differential expression of heme oxygenase-1 in cultured cortical neurons and astrocytes determined by the aid of a new heme oxygenase antibody. Response to oxidative stress. *Brain Res Mol Brain Res*. 1995;30:37–47.
18. Dwyer BE, Nishimura RN, Lu SY, Alcaraz A. Transient induction of heme oxygenase after cortical stab wound injury. *Brain Res Mol Brain Res*. 1996;38:251–259.
19. Ewing JF, Maines MD. Rapid induction of heme oxygenase 1 mRNA and protein by hyperthermia in rat brain: heme oxygenase 2 is not a heat shock protein. *PNAS*. 1991;88:5364–5368.
20. Fukuda K, Panter SS, Sharp FR, Noble LJ. Induction of heme oxygenase-1 (HO-1) after traumatic brain injury in the rat. *Neurosci Lett*. 1995;199:127–130.
21. Fukuda K, Richmon JD, Sato M, Sharp FR, Panter SS, Noble LJ. Induction of heme oxygenase-1 (HO-1) in glia after traumatic brain injury. *Brain Res*. 1996;736:68–75.
22. Gaasch JA, Lockman PR, Geldenhuys WJ, Allen DD, Van der Schyf CJ. Brain iron toxicity: differential responses of astrocytes, neurons, and endothelial cells. *Neurochem Res*. 2007;32:1196–1208.
23. Gardner AJ, Zafonte R. Neuroepidemiology of traumatic brain injury. *Handb Clin Neurol*. 2016;138:207–223.
24. Ginhoux F, Lim S, Hoeffel G, Low D, Huber T. Origin and differentiation of microglia. *Front Cell Neurosci*. 2013;7:45.
25. Giza CC, Hovda DA. The new neurometabolic cascade of concussion. *Neurosurgery*. 2014;75:S24–S33.
26. Ham D, Schipper HM. Heme oxygenase-1 induction and mitochondrial iron sequestration in astroglia exposed to amyloid peptides. *Cell Mol Biol*. 2000;46:587–596.
27. Jullienne A, Salehi A, Affeldt B, et al. Male and female mice exhibit divergent responses of the cortical vasculature to traumatic brain injury. *J Neurotrauma*. 2018;35:1646–1658.
28. Kitamuro T, Takahashi K, Ogawa K, et al. Bach1 functions as a hypoxia-inducible repressor for the heme oxygenase-1 gene in human cells. *J Biol Chem*. 2003;278:9125–9133.
29. Krieg SM, Voigt F, Knuefermann P, Kirschning CJ, Plesnila N, Ringel F. Decreased secondary lesion growth and attenuated immune response after traumatic brain injury in Tlr2/4(-/-) mice. *Front Neurol*. 2017;8:455.
30. Langlois JA, Rutland-Brown W, Wald MM. The epidemiology and impact of traumatic brain injury: a brief overview. *J Head Trauma Rehabil*. 2006;21:375–378.
31. Lee JB, Affeldt BM, Gamboa Y, et al. Repeated pediatric concussions evoke long-term oligodendrocyte and white matter microstructural dysregulation distant from the injury. *Dev Neurosci*. 2018;40:358–375. https://doi.org/10.1159/000494134.
32. Lee PJ, Jiang BH, Chin BY, et al. Hypoxia-inducible factor-1 mediates transcriptional activation of the heme oxygenase-1 gene in response to hypoxia. *J Biol Chem*. 1997;272:5375–5381.
33. Li Volti G, Wang J, Traganos F, Kappas A, Abraham NG. Differential effect of heme oxygenase-1 in endothelial and smooth muscle cell cycle progression. *Biochem Biophys Res Commun*. 2002;296:1077–1082.
34. Li Volti G, Ientile R, Abraham NG, et al. Immunocytochemical localization and expression of heme oxygenase-1 in primary astroglial cell cultures during differentiation: effect of glutamate. *Biochem Biophys Res Commun*. 2004;315:517–524.
35. Lin Q, Weis S, Yang G, et al. Heme oxygenase-1 protein localizes to the nucleus and activates transcription factors important in oxidative stress. *J Biol Chem*. 2007;282:20621–20633.
36. Liu Y, Zhang Z, Luo B, Schluesener HJ, Zhang Z. Lesional accumulation of heme oxygenase-1+ microglia/macrophages in rat traumatic brain injury. *NeuroReport*. 2013;24:281–286.
37. Mannaioni PF, Vannacci A, Masini E. Carbon monoxide: the bad and the good side of the coin, from neuronal death to anti-inflammatory activity. *Inflammation Res: Off J Eur Histamine Res Soc [et al]*. 2006;55:261–273.
38. Matsuoka Y, Kitamura Y, Okazaki M, et al. Kainic acid induction of heme oxygenase in vivo and in vitro. *Neuroscience*. 1998;85:1223–1233.
39. McCoubrey Jr WK, Huang TJ, Maines MD. Isolation and characterization of a cDNA from the rat brain that encodes hemoprotein heme oxygenase-3. *Eur J Biochem*. 1997;247:725–732.
40. Naidu S, Wijayanti N, Santoso S, Kietzmann T, Immenschuh S. An atypical NF-kappa B-regulated pathway mediates phorbol ester-dependent heme oxygenase-1 gene activation in monocytes. *J Immunol*. 2008;181:4113–4123.
41. Nimura T, Weinstein PR, Massa SM, Panter S, Sharp FR. Heme oxygenase-1 (HO-1) protein induction in rat brain following focal ischemia. *Brain Res Mol Brain Res*. 1996;37:201–208.
42. Orihara Y, Tsuda R, Ikematsu K, Nakasono I, Ogata M. Immunohistochemical study on the induction of heme oxygenase-1 by traumatic brain injury. *Leg Med*. 2003;5:S278–S279.
43. Otterbein LE, Bach FH, Alam J, et al. Carbon monoxide has anti-inflammatory effects involving the mitogen-activated protein kinase pathway. *Nat Med*. 2000;6:422–428.
44. Ozen M, Zhao H, Lewis DB, Wong RJ, Stevenson DK. Heme oxygenase and the immune system in normal and pathological pregnancies. *Front Pharmacol*. 2015;6:84.
45. Parfenova H, Basuroy S, Bhattacharya S, et al. Glutamate induces oxidative stress and apoptosis in cerebral vascular endothelial cells: contributions of HO-1 and HO-2 to cytoprotection. *Am J Physiol Cell Physiol*. 2006;290:C1399–C1410.
46. Park C, Cho IH, Kim D, et al. Toll-like receptor 2 contributes to glial cell activation and heme oxygenase-1 expression in traumatic brain injury. *Neurosci Lett*. 2008;431:123–128.
47. Puntambekar SS, Saber M, Lamb BT, Kokiko-Cochran ON. Cellular players that shape evolving pathology and neurodegeneration following traumatic brain injury. *Brain Behav Immun*. 2018;71:9–17.
48. Richmon JD, Fukuda K, Maida N, et al. Induction of heme oxygenase-1 after hyperosmotic opening of the blood-brain barrier. *Brain Res*. 1998;780:108–118.

49. Salehi A, Jullienne A, Baghchechi M, et al. Up-regulation of Wnt/beta-catenin expression is accompanied with vascular repair after traumatic brain injury. *J Cereb Blood Flow Metab: Off J Int Soc Cereb Blood Flow Metab*. 2018;38:274–289.
50. Schallner N, Pandit R, LeBlanc 3rd R, et al. Microglia regulate blood clearance in subarachnoid hemorrhage by heme oxygenase-1. *J Clin Investig*. 2015;125:2609–2625.
51. Sofroniew MV, Vinters HV. Astrocytes: biology and pathology. *Acta Neuropathol*. 2010;119:7–35.
52. Steiner J, Bernstein HG, Bielau H, et al. Evidence for a wide extra-astrocytic distribution of S100B in human brain. *BMC Neurosci*. 2007;8:2.
53. Stocker R, Yamamoto Y, McDonagh AF, Glazer AN, Ames BN. Bilirubin is an antioxidant of possible physiological importance. *Science*. 1987; 235:1043–1046.
54. Tenhunen R, Marver HS, Schmid R. Microsomal heme oxygenase. Characterization of the enzyme. *J Biol Chem*. 1969;244:6388–6394.
55. Villapol S, Byrnes KR, Symes AJ. Temporal dynamics of cerebral blood flow, cortical damage, apoptosis, astrocyte-vasculature interaction and astrogliosis in the pericontusional region after traumatic brain injury. *Front Neurol*. 2014;5:82.
56. Wang J, Dore S. Heme oxygenase-1 exacerbates early brain injury after intracerebral haemorrhage. *Brain: J Neurol*. 2007;130:1643–1652.
57. Werner C, Engelhard K. Pathophysiology of traumatic brain injury. *Br J Anaesth*. 2007;99:4–9.
58. Xiong Y, Mahmood A, Chopp M. Animal models of traumatic brain injury. *Nat Rev Neurosci*. 2013;14:128–142.
59. Yi JH, Hazell AS. N-acetylcysteine attenuates early induction of heme oxygenase-1 following traumatic brain injury. *Brain Res*. 2005;1033:13–19.
60. Yu X, Song N, Guo X, Jiang H, Zhang H, Xie J. Differences in vulnerability of neurons and astrocytes to heme oxygenase-1 modulation: Implications for mitochondrial ferritin. *Sci Rep*. 2016;6:24200.
61. Zhang Z, Zhang ZY, Wu Y, Schluesener HJ. Immunolocalization of Toll-like receptors 2 and 4 as well as their endogenous ligand, heat shock protein 70, in rat traumatic brain injury. *NeuroImmunoModulation*. 2012;19:10–19.